Self-Consistent Simulations of Standard *H*-Mode ITER with the Presence of an Internal Transport Barrier

B. Chatthong, and T. Onjun
School of Manufacturing Systems and Mechanical Engineering, Sirindhorn International Institute of Technology, Thammasat University, Pathum Thani, Thailand

Abstract

Self-consistent simulations of standard *H*-mode ITER with the presence of an internal transport barrier (ITB) are carried out using BALDUR integrated predictive modelling code with predictive models for transport, boundary conditions, and toroidal velocity. In these simulations, the boundary is taken to be at the top of the pedestal. This boundary model is based on a combination of magnetic and flow shear stabilization pedestal width scaling and an infinite-n ballooning pressure gradient model. For the plasma core, a combination of semi-empirical Mixed Bohm/gyro-Bohm (Mixed B/gB) anomalous transport model that includes ITB effects and NCLASS neoclassical transport model is used. In the anomalous transport model, the turbulence is suppressed by the effects of ω_{ExB} flow shear, and magnetic shear, which can automatically trigger a formation of ITB. The toroidal velocity for estimating ω_{ExB} in the ITB prediction is calculated using an empirical approach model that is directly proportional to local ion temperature. The combination of Mixed B/gB core transport model with ITB effects, together with the pedestal and the toroidal velocity models, is used to predict the time evolution of plasma temperature and density profiles of standard type I ELMy *H*-mode ITER performance. It is found that the simulations show a formation of ITB. In addition, the central ion temperature, total fusion power output, and alpha power are approximately 50 keV, 800 MW and 220 MW, respectively.

Keywords: Internal Transport Barrier; *H*-mode; Toroidal Velocity; BALDUR

1. Introduction

Progress in nuclear fusion research has been actively made over the past 50 years in bringing fusion energy to be an alternative energy source for our future. Magnetic confinement fusion devices such as a Tokamak, are the most successfully developed experimental machines from scientific and engineering perspectives, for a fusion reaction control system. The International Thermonuclear Experimental Reactor (ITER) is an international collaboration with the main goal to demonstrate scientific and engineering possibilities of nuclear fusion [1]. The machine will be

ready for experiments approximately 2020 aiming to be a prototype reactor for electricity production. To produce significant fusion reactions inside a tokamak, high plasma temperature and density, as well as a sufficient energy confinement time, are required. Since the high confinement mode (*H*-mode) plasmas in tokamaks generally provide high temperature and excellent energy confinement time, burning fusion experiments such as ITER are designed to operate in the *H*-mode regime. It is known that the improved performance of *H*-mode mainly results from the formation of an edge transport barrier (ETB) [2], called the pedestal. The performance of an *H*-mode discharge can be improved even further with the formation of a transport barrier inside the plasma, called an internal transport barrier (ITB) [3]. The presence of both ETB and ITB in the plasma causes major improvement in core temperature, pressure, confinement time, and hence, fusion power production.

In the last 10 years or so, there has been much research carried out on the predictions of ITER performance in the standard type I ELMy *H*-mode using different integrated predictive modeling codes [4-8]. The core transport models used in those simulations are Mixed Bohm/gyro-Bohm (Mixed B/gB), MMM95, and GLF23 running under different predictive modeling codes such as BALDUR, JETTO, PTRANSP, and ASTRA code. The performance of ITER was normally evaluated in terms of total fusion power output, alpha power, and central temperature. Those simulations yielded a wide range of the predictions depending on initial conditions like heating power, plasma density, impurity conditions, or even cross-sectional shape of the plasma. Additionally, the differences were also dependent on the choice of transport model and code implemented in the simulations. Furthermore, in the recent work by Onjun *et al* [9], the simulations of ITER with combined effects of ITB and ETB were carried out to predict performance of ITB *H*-mode plasma.

It is widely believed that ω_{ExB} flow shear is one of the keys of the formation of ITB. The development of the ω_{ExB} flow shear concept to describe the formation of ITBs in magnetic confinement devices is one of the breakthroughs in fusion plasma research [10-11]. The ω_{ExB} flow shear was originally developed to describe the plasma edge during *L-H* mode transition. Then it was modified to explain further improvement of tokamak confinement with transport barriers in the core of the plasma having low or negative magnetic shear [10]. It is found that the reduction of transport is associated with shear effects, especially the velocity shear and magnetic shear [11]. Theoretically, the calculation of ω_{ExB} flow shear requires the toroidal velocity (v_{tor}) as one of the parameters. There have been studies of momentum and velocity transport in poloidal direction [12-15] but not much has been done on toroidal direction. Especially, there is no model yet to explain the toroidal velocity in a simple fashion or an exact form. Simulations in Ref. [9] were done by using experimental data of toroidal velocity from existing tokamaks JET as an input which raises some questions, because ITER is in a much higher regime, so the physics of a toroidal velocity profile might be completely different.

In this paper, BALDUR integrated predictive modeling code is used to simulate the time-evolution profiles of electron density and ion temperature. The *H*-mode ETB model used in this paper is based on Ref. [16]. In this model the ETB is expressed in terms of a pedestal model. This region is the rising pedestal at the edge of plasma and the gradient is assumed to be constant. The pedestal temperature is explained using the theory based pedestal width model combined with pressure gradient limits, with ballooning mode instability. The pedestal width model is

based on magnetic and flow shear stabilization ($\Delta \propto \rho_i s^2$) [17]. The model is found to be in agreement with experimental data around 30% RMSE [16]. The model for ITB used in this paper is based on literature review of ITB (both theoretical work and experimental work). It is called a semi-empirical Mixed B/gB core transport model which proposes that formation of ITB is caused by the suppression in anomalous transport due to ω_{ExB} flow shear and magnetic shear [18]. This model has been found to successfully reproduce the data from various JET experiments [18-23]. In BALDUR, data for ω_{ExB} is given to the code. The code can also use the data taken from experiments. Moreover, ω_{ExB} can be calculated from toroidal velocity v_{tor}, which can also be taken from experiments. Nevertheless, in order to predict a future machine like ITER, it is important to develop a model estimating toroidal velocity. In addition, to be fully self-consistent, it is essential for BALDUR to be able to calculate v_{tor}, and hence, ω_{ExB} from fundamental physics quantities such as geometrical data of each tokamak, density, current, magnetic field, temperature, and etc. This paper focuses on the use of a model for calculating toroidal velocity to combine with ITB and ETB models to predict ITER performance for a standard type I ELMy *H*-mode scenario. The development and testing of a v_{tor} model is extensively discussed in Ref.[24]. The model is developed using an empirical approach similar to that suggested in Ref. [25], in which the toroidal velocity is a function of local ion temperature.

The paper is organized as follows: an introduction to BALDUR code is presented in section 2, along with theory of Mixed B/gB model, pedestal model, and toroidal velocity model; results of simulation and discussion are presented in section 3; and a summary is given in section 4.

2. Description of Codes

2.1 BALDUR

BALDUR integrated predictive modeling code [26] is a time-dependent transport modeling code which is used to compute many physical quantities in tokamaks. The code itself simultaneously solves three diffusion equations of number density, energy density and poloidal magnetic field. The code computes the time evolution profiles of the electron density, electron temperatures, and ion temperature, which are presented here. Moreover, it can be used to compute other physical quantities like impurity and hydrogen densities, magnetic *q* and other gas densities.

BALDUR code self-consistently computes these profiles by mixing many physical processes together in the form of modules, for example, transport, plasma heating, particle flux, boundary conditions, and sawtooth oscillation modules. It was found that results from BALDUR are in agreement with experimental data. For example, BALDUR simulations yielded an agreement of about 10% relative root mean square deviation (RMSD) for both *L*-mode and *H*-mode plasmas [27-28].

2.2 Mixed B/gB model

The physical mechanism of the ITB formation has not yet been clearly identified. However, it is found that the suppression of core anomalous transport due to ω_{ExB} flow shear and magnetic shear causes ITB formations [18, 29]. ITB formation and its dynamics are modelled through a semi-empirical core transport model called Mixed B/gB [19]. This model is a semi-empirical model. It was originally a local transport model with Bohm scaling which means the diffusivities are proportional to the gyro-radius times the thermal velocity. These transport diffustivities are also functions of plasma parameters such as magnetic *q*. So in the simulations, all parameters are fixed, while the gyro-radius

is changed according to plasma dimensions. The Bohm model was at first derived for electron transport for a JET tokamak [30]. Then, it was modified to additionally describe ion transport [31] and a new term called gyro-Bohm was added, in order to simulate results from both smaller and larger tokamaks [32]. Gyro-Bohm scaling essentially means the diffusivities are proportional to the square of the gyro-radius times the thermal velocity divided by the plasma major radius. Usually, the Bohm term dominates over most of the plasma. The gyro-Bohm term contributes mainly in the deep core of the plasma and in small tokamaks with low heating power and low magnetic field. The Mixed B/gB transport model includes ITB effect by having a cut-off in the Bohm term which is a step function of flow shear and magnetic shear. The model can be expressed as the following [19]:

$$\chi_e = 1.0\chi_{gB} + 2.0\chi_B, \quad (1)$$

$$\chi_i = 0.5\chi_{gB} + 4.0\chi_B, \quad (2)$$

$$D_H = D_Z = (0.3+0.7\rho)\frac{\chi_e\chi_i}{\chi_e+\chi_i}, \quad (3)$$

where

$$\chi_{gB} = 5\times10^{-6}\sqrt{T_e}\left|\frac{\nabla T_e}{B_T^2}\right|, \quad (4)$$

$$\chi_B = \chi_{B_0}\times\Theta\left(-0.14+s-\frac{1.47\omega_{E\times B}}{\gamma_{ITG}}\right), \quad (5)$$

with

$$\chi_{B_0} = 4\text{x}10^{-5}R\left|\frac{\nabla(n_eT_e)}{n_eB_T}\right|q^2\left(\frac{T_e(0.8\rho_{max})-T_e(\rho_{max})}{T_e(\rho_{max})}\right), \quad (6)$$

where χ_e is the electron diffusivity, χ_i is the ion diffusivity, χ_{gB} is the gyro-Bohm contribution, χ_B is the Bohm contribution, D_H is the particle diffusivity, D_Z is the impurity diffusivity, ρ is normalized minor radius, T_e is the local electron temperature, B_T is the toroidal magnetic field, s is the magnetic shear, ω_{ExB} is the shearing rate, γ_{ITG} is the linear growth rate, R is the major radius, and n_e is the local electron density. The linear growth rate γ_{ITG} can be calculated as v_{th}/qR, where v_{th} is the electron thermal velocity.

In this work, the ω_{ExB} shearing rate is calculated according to Hahm-Burrell model [33-34],

$$\omega_{ExB} = \left|\frac{RB_\theta^2}{B_T}\frac{\partial(E_r/RB_\theta)}{\partial\psi}\right|, \quad (7)$$

where B_θ is the poloidal magnetic field, Ψ is the poloidal flux, and E_r is the radial electric field, which can be calculated as follows:

$$E_r = \frac{1}{Zen_i}\frac{\partial p_i}{\partial r} - v_\theta B_T + v_{tor}B_\theta \quad (8)$$

where $\frac{\partial p_i}{\partial r}$ is the pressure gradient, v_θ and v_{tor} are the poloidal and toroidal velocities, respectively, n_i is the ion density, Z is the ion charge number and e is the elementary charge. The calculation of toroidal velocity is discussed in section 2.3.

2.3 Toroidal velocity model

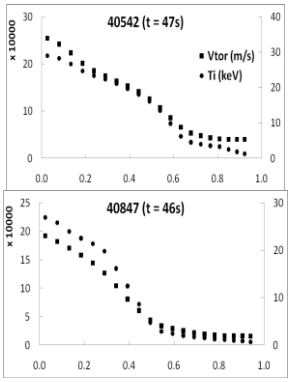

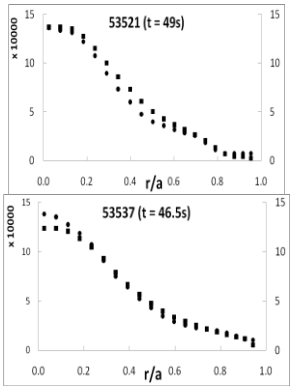

Figure 1 Examples of toroidal velocity (left axis) and ion temperature (right axis) with proper scaling plots as a function of minor radius, at diagnostic times.

This is a simple model based on the idea that toroidal velocity (v_{tor}) is linearly proportional to the local ion temperature (T_i) [25]. Figure 1 shows a correlation between these two physical quantities. The figure also illustrates some examples of toroidal velocity and ion temperature with proper scaling plots as a function of normalized minor radius at diagnostic times. Note that these existing experimental data are taken directly from JET discharges. For full details of development of the model and calculation of the proportional constant, see Ref.[24]. Conclusively, it is found that prior to *L*-*H* mode transition or before Neutral Beam Injection (NBI) is applied to heat the plasma, there is no correlation between the two quantities. However, after the plasma reaches *H*-mode, there is evidently a good linear correlation between the two sets of data. Consequently, this model is implemented only during *H*-mode phase. It is unused during *L*-mode phase and so the toroidal velocity is assumed to be zero. The constant is chosen to be the average of all available data as follows:

$$v_{tor}[m/s] = 1.43\times10^{4} T_i\left[keV\right] \qquad (9)$$

The constant $1.43\text{x}10^4$ in the expression for estimating toroidal velocity is determined by calibrating the model for the toroidal velocity against experimental data points for optimized shear *H*-mode plasmas, obtained from the International Profile Database. This constant minimized the RMSE deviation when the predicted pedestal temperature was compared with the 10260 data points from a total of 10 JET discharges [24].

2.4 Pedestal model

In this study, the boundary conditions are set at the top of the pedestal [35], which is where the edge transport barrier (ETB) is observed. The pedestal region is located at the steep gradient right near the edge of the plasma. It is assumed that the pressure gradient ($\partial p/\partial r$) within this region is constant so the pedestal temperature (T_{ped}) can be calculated as follows [16]:

$$T_{ped} = \frac{1}{2kn_{ped}}\Delta\left|\frac{\partial p}{\partial r}\right| \qquad (10)$$

where n_{ped} (m^{-3}) is pedestal density, k is the Boltzmann's constant, and Δ is the pedestal width. So in order to calculate pedestal temperature, one must obtain pedestal density, pedestal width, and pedestal gradient. In this work, n_{ped} is calculated from experimental data (all JET discharges), while the pressure gradient and width of the pedestal region can be estimated as described below.

The pedestal density, n_{ped}, is obtained by an empirical model which is based on the fact that n_{ped} is a fraction of line average density, n_l, that can be taken from experimental data, as shown:

$$n_{ped} = 0.71 n_l \qquad (11)$$

This pedestal density empirical model agrees with the data from the International Tokamak Physics Activity

(ITPA) pedestal database with 12% RMSE [4].

The pedestal pressure gradient scaling is limited by the ballooning mode instability [36]. It is based on the assumption that there exists a maximum normalized pressure gradient with critical pressure gradient, α_c [16]:

$$\alpha_c(s,\delta,\kappa) = -\frac{2\mu_0 R q^2}{B_T{}^2}\left(\frac{\partial p}{\partial r}\right)_c \qquad (12)$$

Here, κ is elongation, μ_0 is permeability of free space, R is the tokamak major radius, q is safety factor, and B_T is vacuum toroidal magnetic field. Rewrite this relation and substitute the pressure gradient into equation (10) to obtain:

$$T_{ped} = \frac{\Delta}{2kn_{ped}}\frac{\alpha_c B_T{}^2}{2\mu_0 R q^2} \qquad (13)$$

The pedestal width scaling model is based on magnetic and flow shear stabilization ($\Delta \propto \rho_i s^2$) [17]. There is an assumption that the transport barrier is formed in the region where the turbulence growth rate is balanced by a stabilizing $E_r xB$ shearing rate. The scaling width is derived to be [16]:

$$\Delta = C_1 \rho s^2 = C_1\left(4.57x10^{-3}\frac{\sqrt{A_H T_{ped}}}{B_T}\right)s^2, \qquad (14)$$

where C_1 is the constant of proportionality and A_H is the average hydrogenic mass. Combining this scaling with previous pressure gradient scaling, the final T_{ped} is as follows:

$$T_{ped} = C_1^2\left(\left(\frac{4.57x10^{-3}}{4\mu_0(1.6022x10^{-16})}\right)^2\left(\frac{B_T^2}{q^4}\right)\left(\frac{A_H}{R^2}\right)\left(\frac{\alpha_c}{n_{ped}}\right)^2 s^4\right) \qquad (15)$$

This result is used in BALDUR code to calculate the pedestal temperature, which is the boundary condition of the transport model and is used to eventually compute plasma profiles. The constant C_1 is chosen to minimize the RMSD with 533 experimental data points from four large tokamaks obtained from ITPA pedestal database, and from Ref. [16] the constant is found to be 2.42. It is worth noting that this pedestal temperature model includes the effect of edge bootstrap current, which has an impact on magnetic shear and safety factor. This inclusion results in a non-linear behaviour in the pedestal temperature model. The scheme to deal with the approximation of magnetic shear and safety factor for the pedestal prediction using the pedestal models was completely described in reference [16]. Therefore, the values of magnetic shear and safety factor for the pedestal calculation are different from the rest of the values in the BALDUR code, which are based on more appropriate calculations. An attempt to use self-consistent safety factor and magnetic shear for all calculations in BALDUR code is under development. A preliminary result can be seen in Ref. [34]. In addition, there are several new approaches to estimate pedestal values, such as the pedestal scaling by M. Sugihara [17], which predicted the pedestal temperature to be about 5.6 keV.

3. Simulation results and discussion

Table 1: Summary of engineering design parameters for ITER.

Parameters	unit	Full-current
R	m	6.2
a	m	2.0
I_p	MA	15.0
B_T	T	5.3
κ	-	1.7
δ	-	0.33
RF	MW	7.0
NBI	MW	33.0
n_l	m^{-3}	$1.0x10^{20}$

Standard type I ELMy *H*-mode ITER simulations are carried out in this study using BALDUR integrated predictive modeling code. The design parameters are shown in Table 1. Note that δ is triangularity, and RF and NBI represent radio frequency and neutral beam injection heating, respectively. In the simulations, the total run time is 3,000 seconds, of which in the first 100 seconds the plasma current and density are slowly ramped up to designated values. After that, the plasma reaches quasi-steady state with small fluctuations due to numerical error.

3.1 ITB effect on ITER performance

Figure 2 illustrates simulations of ITER for ion temperature (T_i), electron temperature (T_e), deuterium density (n_D), tritium density (n_T), beryllium density (n_{BE}), and helium density (n_{HE}), as a function of normalized minor radius *r/a* at a time of 2,900 seconds. Note that at this time, plasma reaches quasi-steady state conditions. It can be seen in Figure 3 that the plasma becomes relatively steady after 200 seconds. It can be seen in Figure 2 that both temperatures are high near the center and lower toward the edge, while the densities of all species remain roughly the same throughout the plasma except Helium density in ITB simulation, which accumulates near the plasma center.

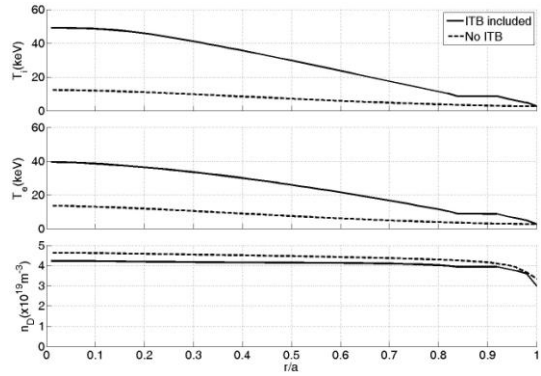

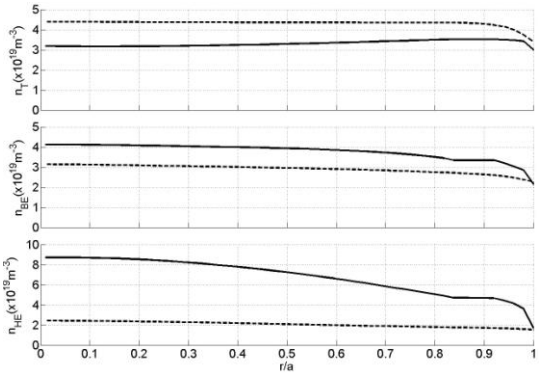

Figure 2 Comparison of ITER performance between with ITB and without ITB effect during steady state (t = 2900 s).

The temperature profiles indicate the existence of ITB formations which are shown by significant improvements of plasma temperature over those results without ITB. It can be seen that when ITB effects are included in the run, the central temperature for both ion and electron increase significantly, from 12 keV to 49 keV and from 13 keV to 39 keV, respectively. Yet, the temperatures near the edge of plasma remain approximately the same. This implies that ITB formations result in better plasma confinement for a plasma temperature, (hence energy). To demonstrate the ITB region, χ_i(ion diffusitivity) and χ_e(electron diffusitivity) are plotted as shown in Figure 4. Both profiles reach a similar conclusion that two ITB regions are formed. The first one extends from plasma center to *r/a* about 0.82, and the second one, a much smaller region, is a bit further out toward the plasma edge. Note that the diffusitivies for ions are higher than that of electron in non ITB regions but lower in ITB regions, this corresponds to ion temperatures being slightly higher than electron temperatures.

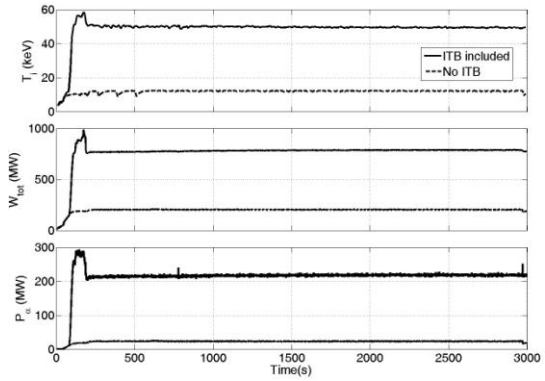

Figure 3 Time-evolution plots of central ion temperature (top), total fusion power output (middle), and alpha power (bottom).

It can be seen that impurities (beryllium and helium) accumulate more in the plasma core for simulation with ITB included, which means that ITB formations also prevent transport of impurity species. Beryllium is an impurity from the first wall outside of the plasma. The concentration is slightly higher in the plasma with the presence of ITB as expected, because there is more beryllium trapped in the core. The situation is similar for helium species, except that the concentration in the run with ITB effect is much higher than the run without ITB effect. As stated earlier, transport barriers improve plasma energy confinement and power production. This means that the fusion reaction rate is enhanced as well. This is confirmed by Figure 3 in the bottom panel which shows time-evolution profile of alpha power. During quasi-steady state, the alpha power of ITB simulation is almost 10 times higher than that when no ITB formed. These alpha particles have charges so they are trapped within the magnetic field inside the tokamak. The energy is then used to reheat the plasma, transferring back to deuterium and tritium by way of collision. More alpha power means more alpha particles produced from fusion reactions, so more helium density is observed. This result is further confirmed by deuterium and tritium densities plots. Since both species are starting particles of fusion reactions, higher reaction rate means more fuel burn and hence less density accumulated for both. As observed in Figure 2, ITB simulation shows less deuterium and tritium concentrations.

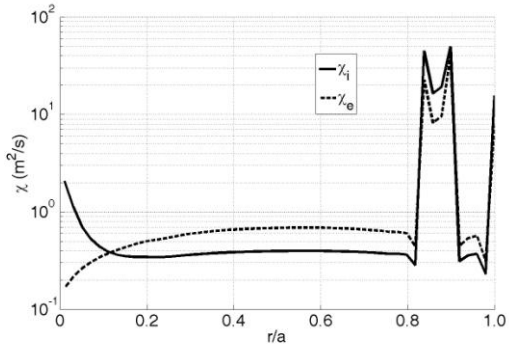

Figure 4 Semi-log plots of diffusion coefficients for ion and electron species at time 2,900 s.

In summary, to see what is happening at the center of the plasma, the central ion temperature is plotted as a function of time (Figure 3) along with total fusion power output and alpha power of the plasma profile plots. As expected, they are higher in simulations, with ITB formation. Initially, during the current ramp-up phase, the profiles increase steeply and reach maximum around 100 seconds before dropping down, because of the high radiation power shown in Figure 5, to reach quasi-steady state. During this latter state, ion temperature reaches a value of 50 keV, the total power output of the plasma is slightly lower than 800 MW, and the alpha power is around 220 MW.

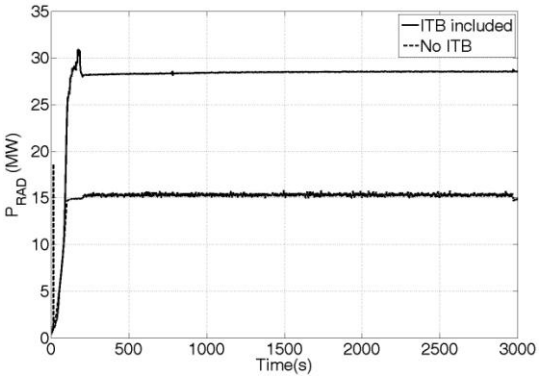

Figure 5 Time-evolution plots of radiation power from the plasma.

3.2 Test of plasma ignition

Plasma reaches ignition conditions when the auxiliary heating (NBI plus RF heating) is shut down, and the plasma still sustains. It is very important to study this issue for ITER because self-heating leads to the possibility of long duration operation for a fusion reactor. In this study, BALDUR code is used to simulate similar ITER performance as before but the auxiliary heating is turned off after 2000 s, at which point the plasma has reached quasi-steady state. After that, the plasma is solely heated by ohmic heating and alpha heating.

It is found in Figure 6 that ion temperature, total power and alpha power drop as soon as the external heating is shut down. Nevertheless, the plasma adjusts to a new quasi-steady state shortly after, with lower temperature and power. In simulation with ITB effects excluded, the operation continues for about 400 seconds longer before reaching disruption, because alpha heating diminishes as soon as the auxiliary heating is off, and then ohmic heating carries the operation until it stops. Note that ohmic heating is small compared to other heatings. With ITB effects included, the plasma achieves a new quasi-steady state at an ion temperature of 40 keV, total power of 650 MW, and alpha power of 180 MW. Note that ITB formations are still maintained even after auxiliary heating is turned off as shown in Figure 7. However, there is one more additional transport region over that of the previous case, indicated by peaks at *r/a* equal to 0.18.

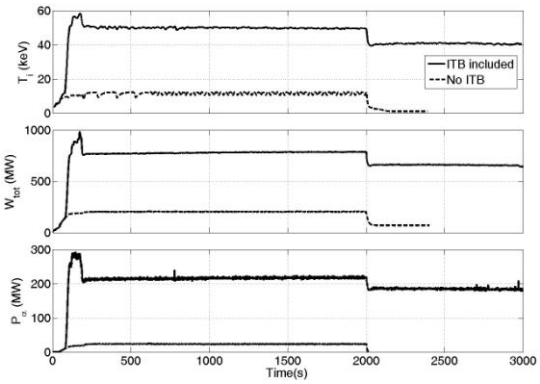

Figure 6 Time-evolution plots of central ion temperature (top), total power output (middle), and alpha power (bottom): Auxiliary heating is turned off after 2000 s.

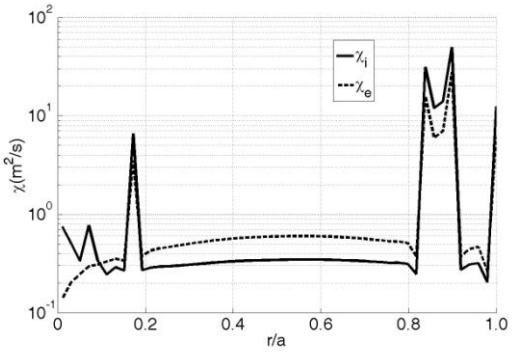

Figure 7 Semi-log plots of diffusion coefficients for ion and electron species at time 2,900 s after auxiliary heating is turned off.

4. Conclusions

Self-consistent simulations of ITER with the presence of both ITB and ETB are done using the BALDUR code. The combination of Mixed B/gB transport model together with pedestal model based on magnetic and flow shear stabilization pedestal width scaling and an infinite-n ballooning pressure gradient model, with empirical toroidal velocity model based on local ion temperature, is used to simulate

the time-evolution profiles of plasma temperature, density, and current for ITER standard type I ELMy *H*-mode operation. The presence of ITB is very crucial because it results in significant improvement of plasma energy confinement over a standard run without ITB effects. The presence of ITB causes both ion and electron temperatures to be higher, especially at the center, but it only slightly affects densities of deuterium, tritium, and beryllium. Helium concentration is higher in ITB simulation because of the increased fusion reaction rate. When the auxiliary heating is turned off, it is found that the core temperature, total power and alpha power decreased slightly. However significant fusion energy is still retained. Ignition conditions cannot be sustained if ITB formations do not exist.

5. Acknowledgments

This work is supported by the Commission on Higher Education (CHE), and the Thailand Research Fund (TRF) under Contract No. RMU5180017. B Chatthong thanks the Royal Thai Scholarship Fund for the scholarship. In addition, we thank Mr.Yutthapong Painroj for ITER information.

6. References

[1] Aymar, R., Barabaschi, P., and Shimomura, Y., The ITER Design, Plasma Phys. Control. Fusion, Vol. 44, No. 5, p. 519, 2002.

[2] Hubbard, A.E., Physics and Scaling of the H-mode Pedestal, Plasma Phys. Control. Fusion, Vol. 42, No. 5A, p. A15, 2000.

[3] Connor, J.W., Fukuda, T., Garbet, X. *et al.*, A review of Internal Transport Barrier Physics for Steady-state Operation of Tokamaks, Nucl. Fusion, Vol. 44, No. 4, p. R1, 2004.

[4] Bateman, G., Onjun, T., and Kritz, A.H., Integrated Predictive Modelling Simulations of Burning Plasma Experiment Designs, Plasma Phys. Control. Fusion, Vol. 45, No. 11, p. 1939, 2003.

[5] Onjun, T., Kritz, A.H., Bateman, G. *et al.*, Magnetohydrodynamic-Calibrated Edge-localized Mode Model in Simulations of International Thermonuclear Experimental Reactor, Phys. Plasmas, Vol. 12, No. 8, p. 082513, 2005.

[6] Halpern, F.D., Kritz, A.H., Bateman, G. *et al.*, Predictive Simulations of ITER Including Neutral Beam Driven Toroidal Rotation, Phys. Plasmas, Vol. 15, No. 6, p. 062505, 2008.

[7] Budny, R.V., Andre, R., Bateman, G. *et al.*, Predictions of H-mode Performance in ITER, Nucl. Fusion, Vol. 48, No. 7, p. 075005, 2008.

[8] Roach, C.M., Walters, M., Budny, R.V. *et al.*, The 2008 Public Release of the International Multi-tokamak Confinement Profile Database, Nucl. Fusion, Vol. 48, No. 12, p. 125001, 2008.

[9] Onjun, T., and Pianroj, Y., Simulations of ITER with combined effects of internal and Edge Transport Barriers, Nucl. Fusion, Vol. 49, No. 7, p. 075003, 2009.

[10] Burrell, K.H., Summary of Experimental Progress and Suggestions for Future Work (H-mode Confinement), Plasma Phys. Control. Fusion, Vol. 36, No. 7A, p. A291, 1994.

[11] Burrell, K.H., Effects of E x B Velocity Shear and Magnetic Shear on Turbulence and Transport in Magnetic Confinement Devices, Phys. Plasmas, Vol. 4, No. 5, p. 1499-1518, 1997.

[12] Tala, T., Crombé, K., Vries, P.C.d. *et al.*, Toroidal and Poloidal Momentum

Transport Studies in Tokamaks, Plasma Phys. Control. Fusion, Vol. 49, No. 12B, p. B291, 2007.

[13] Rozhansky, V., Kaveeva, E., Voskoboynikov, S. *et al.*, Modelling of Electric Fields in Tokamak Edge Plasma and L-H Transition, Nucl. Fusion, Vol. 42, No. 9, p. 1110, 2002.

[14] Rogister, A.L., Rice, J.E., Nicolai, A. *et al.*, Theoretical Interpretation of The Toroidal Rotation Velocity Observed in Alcator C-Mod Ohmic H-mode Discharges, Nucl. Fusion, Vol. 42, No. 9, p. 1144, 2002.

[15] Eriksson, A., Nordman, H., Strand, P. *et al.*, Predictive Simulations of Toroidal Nomentum Transport at JET, Plasma Phys. Control. Fusion, Vol. 49, No. 11, p. 1931, 2007.

[16] Onjun, T., Bateman, G., Kritz, A.H. *et al.*, Models for the Pedestal Temperature at the Edge of H-mode Tokamak Plasmas, Phys. Plasmas, Vol. 9, No. 12, p. 5018-5030, 2002.

[17] Sugihara, M., Igitkhanov, Y., Janeschitz, G. *et al.*, A Model for H mode Pedestal width Scaling Using the International Pedestal Database, Nucl. Fusion, Vol. 40, No. 10, p. 1743, 2000.

[18] Tala, T.J.J., Heikkinen, J.A., Parail, V.V. *et al.*, ITB Formation in Terms of ω E×B Flow Shear and Magnetic Shear s on JET, Plasma Phys. Control. Fusion, Vol. 43, No. 4, p. 507, 2001.

[19] Tala, T.J.J., Parail, V.V., Becoulet, A. *et al.*, Comparison of Theory-based and Semi-empirical Transport Modelling in JET Plasmas with ITBs, Plasma Phys. Control. Fusion, Vol. 44, No. 5A, p. A495, 2002.

[20] Parail, V.V., Baranov, Y.F., Challis, C.D. *et al.*, Predictive Modelling of JET Optimized Shear Discharges, Nucl. Fusion, Vol. 39, No. 3, p. 429, 1999.

[21] Parail, V.V., Energy and Particle Transport in Plasmas with Transport Barriers, Plasma Phys. Control. Fusion, Vol. 44, No. 5A, p. A63, 2002.

[22] Tala, T., Laborde, L., Mazon, D. *et al.*, Predictive Transport Simulations of Real-time Profile Control in JET Advanced Tokamak Plasmas, Nucl. Fusion, Vol. 45, No. 9, p. 1027, 2005.

[23] Tala, T., Imbeaux, F., Parail, V.V. *et al.*, Fully Predictive Time-dependent Transport Simulations of ITB Plasmas in JET, JT-60U and DIII-D, Nucl. Fusion, Vol. 46, No. 5, p. 548, 2006.

[24] Chatthong, B., Onjun, T., and Singhsomroje, W., Model for Toroidal Velocity in H-mode Plasmas in the Presence of Internal Transport Barriers, Nucl. Fusion, Vol. 50, No. 6, p. 064009, 2010.

[25] Kessel, C.E., Giruzzi, G., Sips, A.C.C. *et al.*, Simulation of the Hybrid and Steady State Advanced Operating Modes in ITER, 21st Fusion Energy Conference (Chengdu, China), Paper IT/P1-7, 2006

[26] Singer, C.E., Post, D.E., Mikkelsen, D.R. *et al.*, Baldur: A One-dimensional Plasma Transport Code, Comput. Phys. Commun., Vol. 49, No. 2, pp. 275-398, 1988.

[27] Hannum, D., Bateman, G., Kinsey, J. *et al.*, Comparison of High-mode Predictive Simulations Using Mixed Bohm/gyro-Bohm and Multi-Mode (MMM95) Transport Models, Phys. Plasmas, Vol. 8, No. 3, pp. 964-974, 2001.

[28] Onjun, T., Bateman, G., Kritz, A.H. *et al.*, Comparison of Low Confinement Mode Transport Simulations Using the Mixed Bohm/gyro-Bohm and the Multi-Mode-95 Transport Model, Phys.

Plasmas, Vol. 8, No. 3, pp. 975-985, 2001.

[29] Erba, M., Cherubini, A., Parail, V.V. *et al.*, Development of a Non-local Model for Tokamak Heat Transport in L-mode, H-mode and Transient Regimes, Plasma Phys. Control. Fusion, Vol. 39, No. 2, p. 261, 1997.

[30] Taroni, A., Erba, M., Springmann, E. *et al.*, Global and Local Energy Confinement Properties of Simple Transport Coefficients of the Bohm Type, Plasma Phys. Control. Fusion, Vol. 36, No. 10, p. 1629, 1994.

[31] Erba, M., Parail, V., Springmann, E. *et al.*, Extension of a Bohm Model for L-mode Electron Heat Transport to Ion Heat Transport and to the Ohmic Regime, Plasma Phys. Control. Fusion, Vol. 37, No. 11, p. 1249, 1995.

[32] Erba, M., Aniel, T., Basiuk, V. *et al.*, Validation of a New Mixed Bohm/gyro-Bohm Model for Electron and Ion Heat Transport Against the ITER, Tore Supra and START Database Discharges, Nucl. Fusion, Vol. 38, No. 7, p. 1013, 1998.

[33] Pankin, A.Y., Voitsekhovitch, I., Bateman, G. *et al.*, Combined Model for the H-mode Pedestal and ELMs, Plasma Phys. Control. Fusion, Vol. 47, No. 3, p. 483, 2005.

[34] Zhu, P., Bateman, G., Kritz, A.H. *et al.*, Predictive Transport Simulations of Internal Transport Barriers Using the Multi-Mode model, Phys. Plasmas, Vol. 7, No. 7, pp. 2898-2908, 2000.

[35] Kritz, A.H., Bateman, G., Kinsey, J. *et al.*, The National Transport Code Collaboration Module Library, Comput. Phys. Commun., Vol. 164, No. 1-3, p. 108-113, 2004.

[36] Connor, J.W., A Review of Models for ELMs, Plasma Phys. Control. Fusion, Vol. 40, No. 2, p. 191, 1998.